

On the Effect of Atoms in Solid Solution on Grain Growth Kinetics

EMMANUEL HERSENT, KNUT MARTHINSEN, and ERIK NES

The discrepancy between the classical grain growth law in high purity metals (grain size $D \propto t^{1/2}$) and experimental measurements has long been a subject of debate. It is generally believed that a time growth exponent less than 1/2 is due to small amounts of impurity atoms in solid solution even in high purity metals. The present authors have recently developed a new approach to solute drag based on solute pinning of grain boundaries, which turns out to be mathematically simpler than the classic theory for solute drag. This new approach has been combined with a simple parametric law for the growth of the mean grain size to simulate the growth kinetics in dilute solid solution metals. Experimental grain growth curves in the cases of aluminum, iron, and lead containing small amounts of impurities have been well accounted for.

DOI: 10.1007/s11661-014-2459-y

© The Author(s) 2014. This article is published with open access at Springerlink.com

I. INTRODUCTION

GRAIN growth in crystalline solids occurs by the migration of grain boundaries, where the excess free energy of the boundary structure generates the driving pressure.^[1,2] During normal grain growth, the microstructure changes in a uniform way, there is a narrow range of grain sizes and shapes, and the form of the grain size distribution is independent of time and hence on scale. In pure metals and stable solid solution alloys, the kinetics of normal grain growth during isothermal annealing is in general well described by the following empirical equation:

$$D^n - D_0^n = Kt, \quad [1]$$

where D and D_0 are the instantaneous and the initial average grain sizes, respectively; t is the isothermal annealing time; and K a parameter depending on material and temperature, and the exponent n , which also varies with material and temperature, is usually referred to as the grain growth exponent. It follows from the classical treatment by Burke and Turnbull^[2] that $n = 2$. However, in high purity metals and solid solution alloys, n is usually found to be larger than 2 as illustrated by the results shown in Figures 1 and 2, taken from Gordon and El-Bassyouni^[3] and Hu^[4] on high purity aluminum and zone-refined iron, respectively. In the work by Beck *et al.*^[5] on aluminum

n -values in the range from 3 to 18 were reported. For a review, see Humphreys and Hatherly.^[6]

No generally accepted theory has been developed which accounts for n being larger than 2, but a common belief is that non-linear dependence of velocity on driving pressure due to solute effects is the main cause for this phenomenon. The classical solute-drag theory established by Cahn^[7] and Lücke and Stüwe^[8,9] is of little help in this context (this theory will be referred in following as the CLS theory). In the extremes, *i.e.*, in situations of breakaway or loaded boundaries, it follows that n should be equal to 2. Only in the unstable situation in-between these extremes, deviation in n -values from 2 can be expected. The solute-drag theory, however, has not been developed to a level which makes it possible to predict the relevant n -values in this region of solute-boundary instability. However, the new *statistical solute-pinning approach* to the effect of solute atoms on boundary migration recently developed by the present authors,^[10] and extended to the effect of multiple components highly diluted in solid solution,^[11] is both physically and mathematically more transparent, which opens for a theoretical analysis of grain growth kinetics in dilute solid solutions.

II. MODELING GRAIN GROWTH KINETICS

The simulation of the grain microstructure evolution by phase-field methods looks very promising.^[12–16] Each grain is characterized by a continuous-phase variable whose value is ranging from 0 outside the grain to 1 inside and whose evolution is described by the physical phenomena to be simulated. It has been shown recently by Grönhagen *et al.*^[14] and Kim *et al.*^[15] that solute drag could be taken into account in a manner consistent with the CLS theory by introducing a concentration dependence in the double-well potential in the Gibbs energy expression. Solute drag in non-steady-state conditions (the CLS theory assumes stationary conditions) and abnormal grain growth induced by solute drag have

EMMANUEL HERSENT, Research Engineer, formerly with the Department of Materials Science and Engineering, Norwegian University of Science and Technology (NTNU), 7491 Trondheim, Norway, is now with Gränges Technology AB, 612 33 Finspång, Sweden. KNUT MARTHINSEN, Professor, Deputy Head of Department, and ERIK NES, Professor Emeritus, are with the Department of Materials Science and Engineering, Norwegian University of Science and Technology (NTNU). Contact e-mail: knut.marthinsen@ntnu.no

Manuscript submitted November 4, 2013.

Article published online August 7, 2014

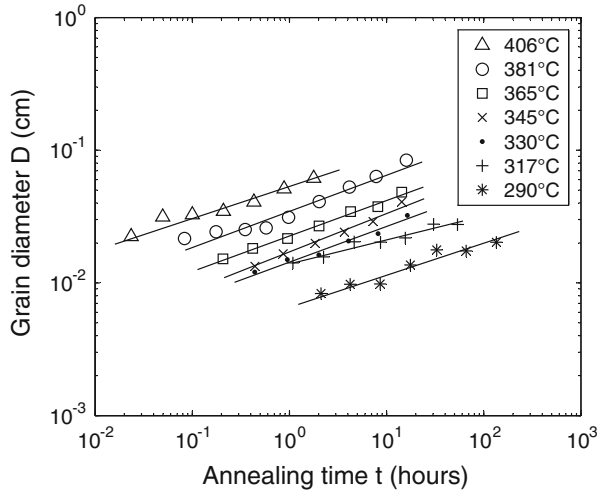


Fig. 1—Grain growth evolution with time in a zone-refined aluminum which has been added 4 ppm Cu (cf. Table I; data redrawn from Ref. [3]). The exponent n averages about 3.4 for the different curves, except for the 590 K (317 °C) curve for which the exponent n equals 5.8.

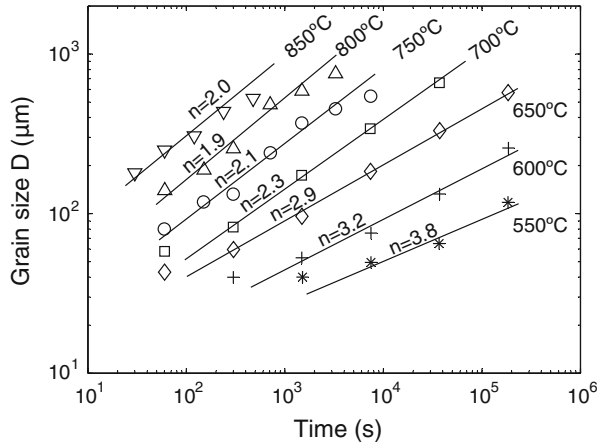


Fig. 2—Grain growth in zone-refined iron during isothermal annealing (data redrawn from Ref. [4]). For each temperature, it has been indicated the value of the exponent n which corresponds to the best fit of the law $D^n = Kt$ to the experimental data (values taken from Fig. 2 in Ref. [4]).

been studied, respectively, in Reference 16 and in Reference 15 with the help of this approach. However, this procedure is computer intensive and as an alternative, it is suggested here to treat grain growth in a simple parametric way, the objective being to define a computational procedure for predicting the time dependence of the average grain size during annealing of a polycrystalline solute containing metal at a constant temperature. It is simply assumed that the growth rate of the average grain size, D , during isothermal annealing at a temperature T will follow a relationship of the form

$$\frac{dD}{dt} = \alpha v_b(c, T, P), \quad [2]$$

where α is a geometric factor depending upon the shape of the grain and $v_b(c, T, P)$ is the steady-state migration rate

of a grain boundary acted upon by a pressure P in a material containing a solute concentration c . In simplistic terms, α can be set equal to 2 as grain boundaries move apart by $v_b dt$. However, the exact value of α is of no consequence since in the present modeling work, α becomes a trivial fitting parameter. In a grain growth situation, the driving pressure is assumed to be well represented by $P = 2\gamma_{GB}/r$, where γ_{GB} is the specific grain boundary energy and r is the grain radius ($r = D/2$). An expression for the boundary migration rate can be found in the solute-pinning analysis referred to above,^[10] and a brief summary of some salient ideas in this approach seems necessary in this context. Further, this summary will also include the equations required in the simulations below.

A. The Solute-Pinning Approach

The migration rate of a high-angle grain boundary in a pure metal at a temperature, T , is commonly given by an expression in the following form^[17]:

$$v_b = mP = \Gamma_p b v_D \frac{Pb^3}{kT} \exp\left(-\frac{U_{SD}^b}{kT}\right). \quad [3]$$

In this equation, m is the boundary mobility, Γ_p is a constant, b is a typical inter-atomic spacing (Burger's vector), v_D is the Debye frequency, k is Boltzmann's constant, and U_{SD}^b is an activation energy associated with boundary migration. This activation energy is typically found to have a value half that of self-diffusion.

If solute atoms are added to the metal, then the situation will change. The present treatment assumes a boundary region potential for the boundary-solute interaction as schematically outlined in Figure 3(a) *i.e.*, $U(x) = -U_0$ for $x(t) - \frac{\lambda}{2} \leq x(t) \leq x(t) + \frac{\lambda}{2}$ and $U(x) = 0$ for all other values of x , where $x(t)$ is the instantaneous position of the boundary and λ is its thickness. Outside the boundary region, thermal activation of the solute atoms is associated with an energy U_s (*i.e.*, that of solute bulk diffusion). With this energy profile, it follows that in the static case, Figure 3(a), the solute atom concentration in the boundary of a material with a solute concentration c will be given by

$$c_b = c \exp\left(\frac{U_0}{kT}\right). \quad [4]$$

If a pressure acts on the boundary, then the boundary may start to migrate and the boundary concentration c_b will change. In the present solute-pinning approach, the basic idea is that the effect of the solute atoms on the boundary migration rate will be determined by the rate at which such atoms are activated out of the boundary region. The pressure P , driving the boundary, results in a cusping force F_C (Figure 3(b)) on each solute atom which reduces the activation barrier out of the boundary by $F_C b$, as illustrated by the energy profile in Figure 3(b). Sometime after the pressure P has been applied, a steady-state boundary-solute concentration c_b will be established, to which corresponds a steady-state boundary migration rate v_b . The statistical treat-

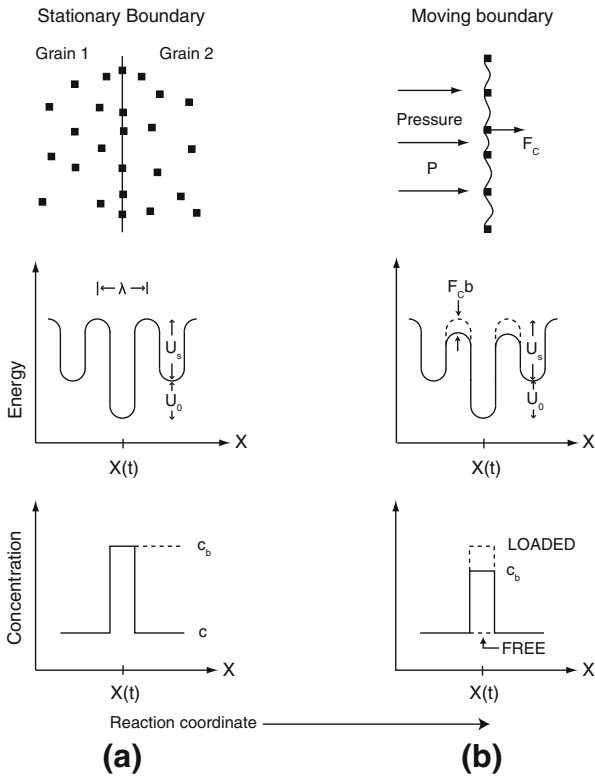


Fig. 3—Schematic representation of the interactions between (a) a stationary and (b) a migrating grain boundary and solute atoms, a simplified version taken from Ref. [10].

ment in Reference 10, balancing thermally activated jump-fluxes into and out of the boundary of the solute, gives the following expressions for the migration rate and boundary-solute concentration

$$v_b = 2\Gamma_s b v_D \exp\left(-\frac{U_s + U_0}{kT}\right) \sinh\left(\frac{F_C b}{kT}\right), \quad [5]$$

$$c_b = c \exp\left(\frac{U_0 - F_C b}{kT}\right) \left[1 + 2 \left(\exp\left(-\frac{U_0}{kT}\right)\right) \sinh\left(\frac{F_C b}{kT}\right)\right]. \quad [6]$$

In order to achieve a complete solution of these equations, an expression for the pinning force F_C is needed, or more exactly for the ratio $\frac{F_C b}{kT}$. Fortunately, it is possible to calculate this force because an alternative expression to Eq. [5] for the migration rate can be formulated, and by having two independent relationships for the same migration rate, the pinning force problem can be solved. This second expression for the boundary speed is obtained by considering a boundary subjected to a driving pressure P and which also experiences a restraining pressure $P_C = F_C/A$, where $A = (1/\lambda c_b n_b)$ is the unit area per boundary atom and n_b is the number of atoms per unit volume in the boundary. In-between these restraining points, the boundary is free of solute atoms with a mobility, m , typical of that of a pure metal, Eq. [3], and it follows that the boundary migration rate also can be written as

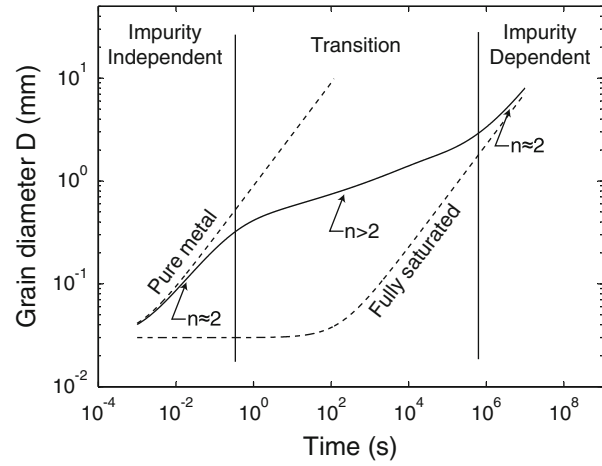


Fig. 4—A typical theoretical evolution of the mean grain size in a generic metallic solid solution.

$$v_b = m(P - P_C). \quad [7]$$

By equating the two expressions for the boundary migration rate, Eqs. [5] and [7], and by replacing m by its expression (Eq. [3]), the pinning force is obtained. Unfortunately, it is not possible to give this force in terms of an analytical expression, only an implicit expression can be given as

$$c = \frac{1}{nb^3} \frac{\left(\frac{Pb^3}{kT} - 2\frac{\Gamma_s}{\Gamma_p} \exp\left(-\frac{U_s + U_0 - U_{SD}^b}{kT}\right) \sinh\left(\frac{F_C b}{kT}\right)\right) \exp\left(\frac{F_C b}{kT}\right)}{\frac{F_C b}{kT} \left(\exp\left(\frac{U_0}{kT}\right) + 2 \sinh\left(\frac{F_C b}{kT}\right)\right)}. \quad [8]$$

However, by numerical treatments, it becomes possible to calculate $F(c, P, T)$, $c_b(c, P, T)$ and $v_b(c, P, T)$ for any given combination of material specific parameters n , b , c , Γ_p , Γ_s , U_{SD}^b , U_0 , and U_s ; for more detail, see Reference 10.

B. Generic Model Predictions

A typical grain growth evolution in a generic solid solution alloy is illustrated in Figure 4. The metal considered is assumed to have a grain boundary energy γ_{GB} of the magnitude 0.5 J/m^2 , an atomic spacing b equal to 3 \AA (typical values in metals), and a solute content of 1 ppm. The atomic density n is estimated as $\frac{1}{b^3}$. The values of the others parameters needed for the simulations are summarized in Table II under the Case A. As illustrated in Figure 4, the grain growth reaction during isothermal annealing can be divided into three stages: (i) An impurity independent regime characterized by conditions where $F_C b/kT \gg 1$ (or breakaway situation). During this period, the time exponent n is nearly equal to 2. (ii) A transition regime during which the growth rate is reduced. The time exponent is larger or much larger than 2. (iii) A final third stage where grain growth has caused a reduction in driving pressure so that $F_C b/kT \ll 1$ (the boundary is fully loaded), and

thus the time exponent n again approaches a value close to 2.

For different values of the interaction energy U_0 , grain boundary migration and grain growth rates have been calculated, Figures 5(a) and (b): The steady-state boundary migration rate (under constant driving pressure P) as a function of solute concentration is illustrated qualitatively in Figure 5(a); grain growth during isothermal annealing at 773 K (500 °C) with a solute content of 1 ppm is illustrated in Figure 5(b). One can note that for values of U_0 larger than some critical level, the v_b vs c curves become S -shaped as illustrated by the broken lines in Figure 5(a). A similar behavior is predicted also by the CLS theory and is there interpreted as an instability phenomenon associated with either breakaway or loading. The physics behind this peculiar behavior is more transparent in the solute-pinning treatment where the breakaway/loading phenomenon is reduced to a well-defined discontinuity (fully drawn lines), the reason for which is argued for in free energy terms. In contrast to the CLS theory, a strong solute-pinning effect may prevail even in cases where the interaction energy $U_0 = 0$. It appears as intuitively obvious that in cases where the activation energy for solute diffusion in the boundary is significantly different from that of boundary self-diffusion, the solute atoms will disturb the solvent redistribution pattern and restrict boundary migration even if the “long range” elastic interaction is negligible. A similar U_0 -effect is found in the model by Westengen and Ryum.^[18] The abrupt drops in boundary velocity for interaction energies above a critical level in Figure 5(a) reappear as plateaus in the growth rates in Figure 5(b). Figure 5(c) illustrates how these curves change in shape with changes in temperature, where the three different stages outlined in Figure 4 can easily be observed especially at the highest temperatures.

III. APPLICATIONS

Grain growth in a zone-refined iron has been studied by Hu^[4] (Figure 2). The material used for this study is a 99.99 pct pure iron containing as impurity C, O, and N amounted to about 30 ppm, and the other impurities being mainly Si, Co, Cr, and Ni. As non-metallic impurities diffuse much faster than metallic impurities, it is expected that only the latter ones can influence the grain growth. Unfortunately, our model is not yet developed to the point where it can take into account the influence of the different impurities, where only the influence of the total amount can be described. The total level of impurity c is, as a best guess, taken as 70 ppm. The activation energy for diffusion U_s of metallic impurities in α -iron ranges from 226 kJ/mol for Co to 358 kJ/mol for Ni,^[19] so 250 kJ/mol is taken as a representative value of this range in this work. Grain boundary energy is generally deduced from zero-creep experiments: one typical set up is to suspend a mass to a thin wire of the studied material put in a furnace and to record the strain rate. From different experiments, it is then possible to extrapolate the mass that gives a zero

strain rate, and thus estimate the grain boundary energy. To get relevant values, it is necessary to carry out the experiments at high enough temperatures in order to assume that the grain boundary energy is independent of the area: $d\gamma_{GB}/dA = 0$, *i.e.*, that atomic diffusion is rapid enough to adapt for the increase or decrease of the grain boundary area. Thus, it seems that it is not possible with this method to estimate experimentally the grain boundary energy of α -Fe due to the allomorphic transformation of iron $\alpha \rightarrow \gamma$ at 1185 K (912 °C). Only theoretical values by atomistic simulations seem available. Values have been computed for different configurations of grain boundaries and ranges typically from 0.8 to 1.4 J/m².^[20–22] In the present work, we have used an average value of 1.0 J/m². The activation energy for boundary migration is often close to that for solvent diffusion in grain boundary (p. 135 in Reference 6), which in the case of α -Fe equals 174 kJ/mol. A value of 167 kJ/mol has been adopted for activation energy for boundary migration in α -Fe in the present work. Finally, the value of Γ_s is adjusted so that the simulation results match as closely as possible the experimental ones. The values of the other parameters needed for the simulations are reported in Table II under the Case B. As illustrated in Figure 6, the experimental observations are well accounted for by the present model.

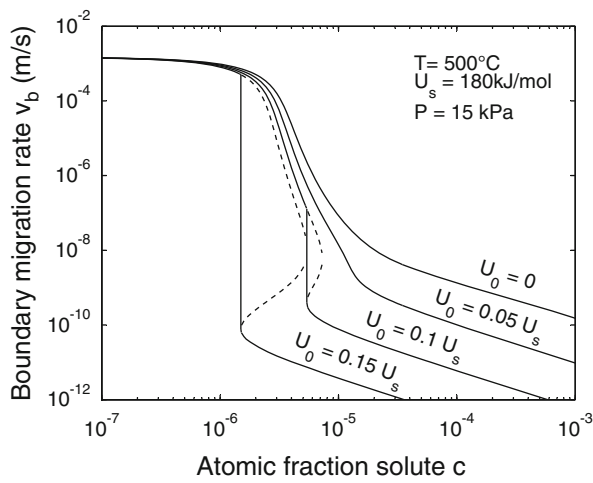
A. Grain Growth in High Purity Aluminum and the Effects of Iron and Manganese in Solid Solution

Many studies over the years have focused on grain growth in dilute aluminum solid solutions, and of particular interest, in this context has been the effect of small quantities of iron and manganese on grain growth kinetics.^[3,5,23–26] An important work in this connection is that by Boutin who carried out a systematic study of the effects of different elements on boundary migration in commercial high purity aluminum (99.99 pct Al) and showed that the migration rate is mainly determined by the iron content, while most other elements,* with the exception of beryllium and

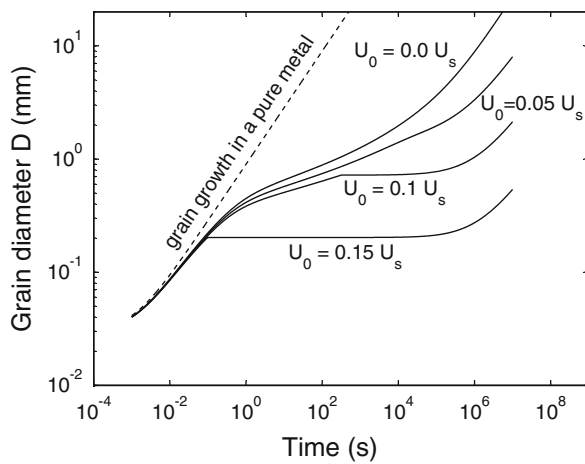
*The effect of the following elements was studied by Boutin in Reference 24: Be, Mg, Si, Ca, Co, Ni, Cu, Zn, Ga, In, Bi, Ti, V, Cr, Nb, Mo, Hf, Ta, W, Zr.

zirconium, do have no or limited effect.^[24] Boutin, however, studied the migration of grain boundaries during primary recrystallization which implies that only qualitative predictions can be drawn from his work regarding the effect of various elements in solid solution on grain growth.

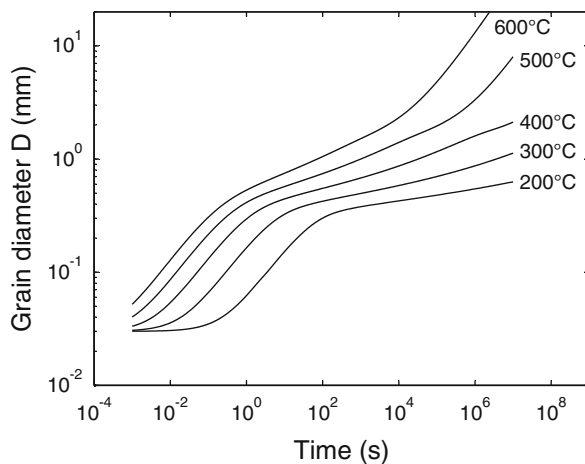
To simulate the effect of Fe on the boundary migration rate during grain growth in high purity aluminum in particular, it is essential that the iron concentration in solid solution could be assumed constant during the different isothermal treatments, which limits the iron content to a few ppm as iron have a very low solubility in aluminum, typically less than 1 ppm. For example, Boutin in his work^[24] observed precipitation of Al₃Fe in his commercial high purity aluminum



(a)



(b)



(c)

Fig. 5—(a) Model predictions for the migration rate v_b with the solute concentration c under a constant driving pressure $P = 15$ kPa at 773 K (500 °C), for the U_0 -values given. (b) Theoretical grain growth evolution curves in a model metal containing 1 ppm of solute at 773 K (500 °C) for different segregation energies U_0 . (c) Model predictions for the grain growth evolution with time in a model metal containing 1 ppm of solute at different temperatures for a solute segregation energy $U_0 = 0.05 U_s$.

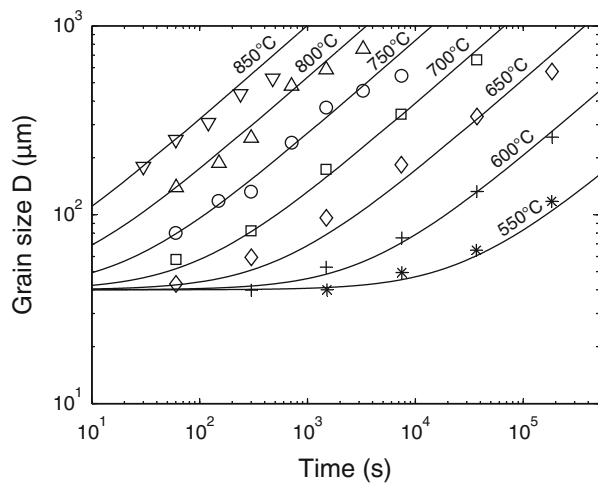


Fig. 6—Experimentally and theoretically predicted variation in grain size in a zone-refined iron with time. The experimental data are taken from Hu.^[4]

which contained about 10 ppm Fe. This observation limits the choice of works to those concerning zone-refined aluminum. In the present work, we therefore focus our attention on the experimental results reported by Gordon and El-Bassyouni,^[3] who studied grain growth in both zone-refined aluminum and zone-refined aluminum containing various additions of copper in the range of 4 to 400 ppm. In the pure zone-refined variant, a surprising observation was a nearly complete stagnation in grain growth below 486 K (213 °C). Another interesting observation was that in the copper containing variants, the copper additions apparently had only marginal effect on grain growth kinetics. Accordingly, these variants also lend themselves to analyzing the effects of the reported iron and manganese contents on grain growth kinetics in these variants. Finally, an interesting objective becomes to investigate if the absence of any copper effect on grain growth is consistent with modeling predictions.

1. Zone-refined aluminum

The quality investigated by Gordon and El-Bassyouni contained in total about 3.5 ppm of detectable trace elements whose composition is reported in Table I. It is not expected that Si or Ti can influence grain growth kinetics, the former because of a too high diffusion coefficient and the latter because of a too low one. One could note that the zone-refined aluminum contained as high as 0.44 ppm Mn. The effect of Mn in solid solution on mechanical properties and recrystallization in aluminum is similar to or may even be stronger than that of Fe, as reported by Ryen *et al.*,^[27] Furu,^[28] and Nes and Furu.^[29] Moreover, the mass-spectrograph analysis of Gordon and El-Bassyouni^[3] was reported to be accurate only to a factor of about 2 to 3. So for the present calculations, it has been decided to take the level Mn equal to be 1 ppm. The activation energy for solute diffusion for Mn was taken equal to 220 kJ/mol, which is a slightly larger value than the one assessed by Du

Table I. Mass-Spectrograph Analyses of Zone-Refined Aluminum Samples and Dilute Copper in Aluminum Alloys (Analyses are Given in Atomic Parts Per Millions)

Element	Zone-Refined Al			
	Unalloyed	+ 4 ppm Cu	+ 40 ppm Cu	+ 400 ppm Cu
Si	1.92	1.74	1.25	4.25
Ca	0.67	0.67	0.41	0.14
Ti	0.28	0.34	0.28	0.84
Mn	0.44	0.44	0.44	0.69
Fe	0.05	0.72	0.24	1.45

The data are taken from Table II in Ref. [3].

Table II. Value of the Parameters Used for the Simulations: (Case A) in a Generic Metallic Solid Solution, Fig. 5(a) Through (c); (Case B) in Zone-Refined Iron, Fig. 6; (Case C) in an Unalloyed Zone-Refined Aluminum, Fig. 7; (Case D) Grain Growth Kinetic Assumed Influenced Only by the Diffusion of Cu, Fig. 9 (For This Case, the Data are Taken from Ref. 10); (Case E) Grain Growth Kinetic Assumed Limited by the Diffusion of Fe and Mn, Fig. 10 (Case F) in Zone-Refined Lead, Fig. 11

	Case A	Case B	Case C	Case D	Case E	Case F
Initial grain size D_0 (μm)	40	40	50	50	50	200
Close spaced atomic spacing b (\AA)	3	2.48	2.86	2.86	2.86	4.950
Grain boundary energy γ_{GB} (J/m^2)	0.5	1.0	0.324*	0.324*	0.324*	0.2
Prefactor Γ_p	150	2.1×10^5	3.9×10^5	3.9×10^5	3.9×10^5	2×10^3
Activation energy for boundary migration U_{SD}^b (kJ/mol)	60	167	65	65	65	25
Estimated impurity content (ppm)	—	70	1	400	3	0.14
Prefactor Γ_s	1	2.5×10^3	1.0×10^6	1.8×10^5	1.0×10^6	0.15
Activation energy for solute diffusion U_s (kJ/mol)	180	250	220	125	220	180
Interaction energy U_0 (kJ/mol)	—	6	6	3	6	6
Fitting parameter κ	1	1	1	0.4	1	1

*p. 104 in Ref. [6].

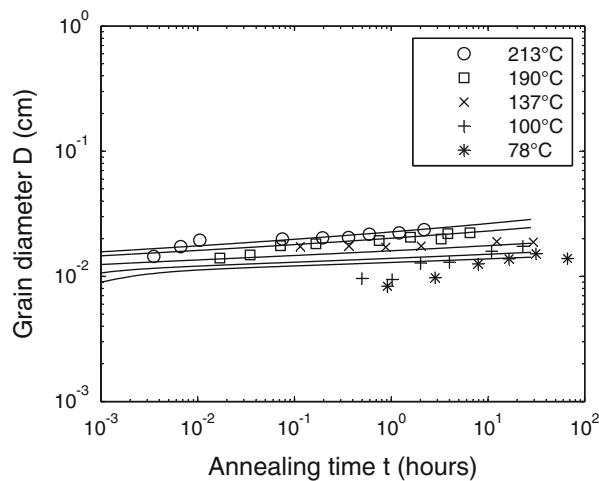


Fig. 7—Experimental and simulated evolutions in grain size with time at different temperatures for an unalloyed zone-refined aluminum alloy. The experimental points are taken from Fig. 4 in Ref. [3]. The simulated curves are obtained by assuming a Mn content of 1 ppm and $D_0 = 50 \mu\text{m}$.

et al. in Reference 30. The interaction energy U_0 was estimated as suggested by Lücke and Detert^[23] as the interfacial energy γ_{GB} times the area of one atom $\frac{a^3}{4\sqrt{2}a}$ (a being the lattice parameter of aluminum) divided by 2 (the interfacial energy is shared by the two adjacent

grains). In the case of aluminum, it gives an estimate of the interaction energy U_0 of about 6 kJ/mol. It should also be noted that the values of the parameters describing the behavior of a pure metal Γ_p and U_{SD}^b are taken from Reference 10. The initial grain size D_0 was taken equal to $50 \mu\text{m}$ (it is reported in Reference 3 that the initial grain size ranges from 30 to $70 \mu\text{m}$). The other parameters needed for the simulations are reported in Table II under the case C. In the temperature range investigated, a near stagnation of growth is predicted, which corresponds well to the experimental observations, see Figure 7.

2. Zone-refined aluminum containing copper

That even additions as high as 400 ppm of Cu have only a minor effect on the grain growth, kinetics is clearly demonstrated by the experimental data outlined in Figure 8, where grain growth curves for a zone-refined aluminum containing 400 ppm Cu can hardly be distinguished from those for a zone-refined aluminum with 4 ppm copper at least for temperatures below 723 K (450 °C). This lack of a copper effect can also be revealed in modeling terms as illustrated by the set of lines representing model predictions of grain growth in a binary Al-400 ppm Cu alloy at temperatures similar to those given in Figure 9 for the experiments and with a corresponding initial grain size of $50 \mu\text{m}$. These lines have been generated based on data derived from the detailed experimental analysis of the effect of copper on grain

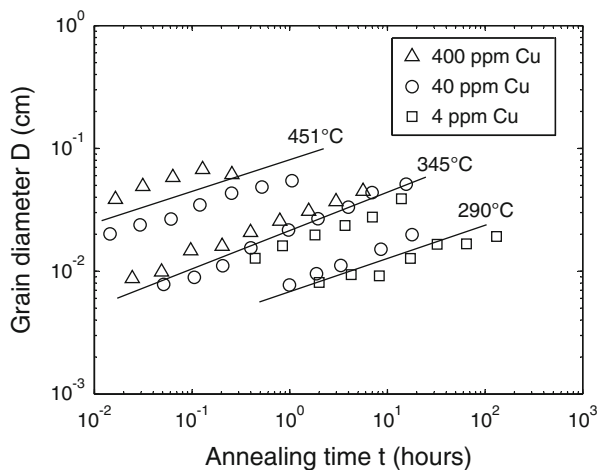


Fig. 8—Superimposed grain growth data for three zone-refined aluminum alloys containing different levels of Cu content at three temperatures (figure redrawn from Fig. 5 in Ref. [3]).

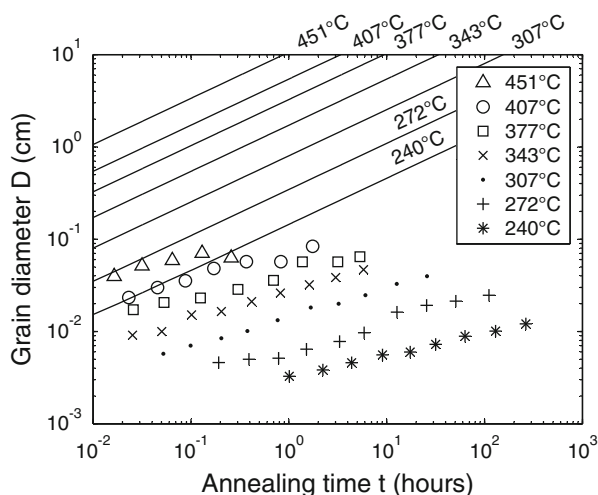


Fig. 9—Model predictions of the evolution in grain size (straight lines) with time at different temperatures for a zone-refined aluminum alloy, with addition of 400 ppm Cu assumed to control the grain growth. Experimental data (with 400 ppm Cu) from Fig. 1 in Ref. [3] are included for comparison.

boundary migration in aluminum by Gordon and Vandermeer^[31] and the model analysis of these data by the present authors.^[10] The values of the different parameters are reported in Table II under the Case D. It should be noted that in the former analysis, a fitting parameter κ was introduced in order to reproduce correctly the variations of the boundary migration rate with the amount of copper obtained by Gordon and Vandermeer. As to estimate the influence of copper on grain growth evolution, this parameter has been reintroduced in Eq. [7]. For all temperatures analyzed, the model curves reflect fully loaded conditions ($n = 2$) and growth rates more than an order of magnitude larger than corresponding experimental ones. In this way, the modeling results underscore the conclusion drawn from the experimental results that any copper effect can be ignored. The addition of copper, however, brings with it some iron and manganese (Table I), and it follows that in

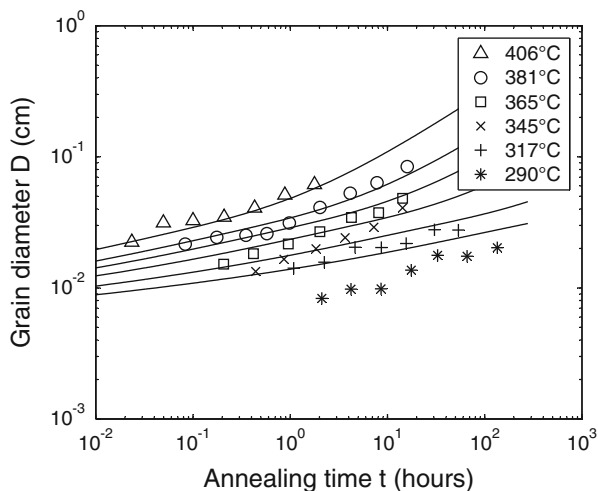


Fig. 10—Experimental and simulated evolutions in grain size with time at different temperatures for an aluminum alloy containing copper. The experimental points are obtained using a zone-refined aluminum, which has been added 4 ppm Cu.^[3] The simulated curves are obtained by considering that iron and manganese are more potent in slowing grain growth than copper and in a total amount of 3 ppm and $D_0 = 50 \mu\text{m}$.

the modeling of the grain growth evolution in the copper containing variants, focus should be directed toward their effects, even if present only in minute quantities.

The activation energy for iron covers a similar range to that given here for manganese,^[30] and it follows that within the framework of the present model, the drag effect due to these two types of solutes in aluminum could not be distinguished from each other. So, the activation energy for Fe/Mn diffusion in aluminum was taken as mentioned earlier equal to $U_s = 220 \text{ kJ/mol}$, and the iron and manganese content in solid solution has been estimated to be 3 ppm. The values of the other parameters needed for the simulations are given in Table II under the Case E. The model correctly predicts nearly straight lines within the range of observations and with n -values within the experimental scatter, see Figure 10. Yet, it should be noted that the model curves slightly deviates upward for the temperatures 590 K to 638 K (317 °C to 365 °C). Moreover, it fails in the prediction of the 563 K (290 °C) results. The experimental observations are lower than expected from the trend resulting from the observations from the other temperatures. It may be, as suggested by Saimoto and Jin,^[26] that at this low temperature, the growth kinetics may be influenced by precipitation. All in all, the simulated grain growth evolutions are fairly well in agreement with those observed.

B. Grain Growth in Zone-Refined Lead

Detailed surveys of grain growth in zone-refined lead have been conducted by Bolling and Winegard^[32,33] and by Drolet and Galibois.^[34,35] The material used presents a very high purity; it was estimated as being at least 99.9999 pct pure. Even in such a pure material, the time exponent n was not measured equal to 2, although it was quite close, *i.e.*, 2.5. Moreover, for annealing times larger than ~ 200 seconds, a decrease in the growth rate

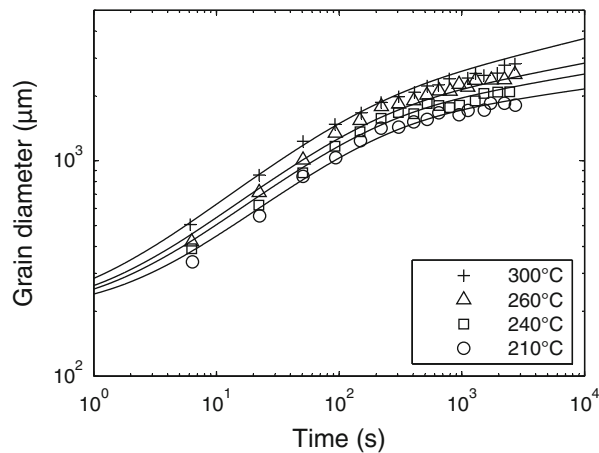


Fig. 11—Experimental and simulated evolutions in grain size with time for different temperatures in a zone-refined lead (experimental data taken from Ref. [33]). The simulated curves are obtained by assuming a solute content of 0.14 ppm; the other parameters needed for the simulations are reported in Table II under Case F.

was observed (Figure 11). Grey and Higgins^[36] interpreted this decrease as a manifestation of a velocity-independent component in the solute drag, maybe due to solute clustering. However, the origin of this component is still unclear, so the original hypothesis, *i.e.*, that this decrease corresponds to a transition behavior from the solute independent regime to the solute dependent regime,^[34,35] was reassessed using our model. The activation energy of the mobility of high-angle boundaries U_{SD}^b was taken as 25 kJ/mol^[37,38] and the grain boundary energy γ_{GB} as 0.2 J/m².^[39] As very pure lead tends to recrystallize at room temperature, the initial grain size D_0 could only be guessed and was taken equal to 200 μm . Experimental observations can be well matched by simulated curves (Figure 11) by taking a solute concentration of 0.14 ppm and an activation energy for solute diffusion U_s of 180 kJ/mol; the other parameters necessary for the simulations are reported in Table II under Case F. Such a low level of solute is in agreement with the fact that the lead was zone refined. However, such high activation energy for solute diffusion in lead is quite uncommon. It is reported in Reference 40 that the activation energy for solute diffusion does not exceed ~ 120 kJ/mol (the tracer impurity diffusion coefficient is not reported for all elements). As no quantitative chemical analysis of the zone-refined lead were carried out, it is difficult to judge if it is really representative of the diffusion of one element or if it is a consequence of other phenomena, like solute clustering. Anyway, our approach indicates that it may not be necessary to introduce a velocity-independent component in the solute drag to interpret these results.

IV. CONCLUDING REMARKS

Even if the model is based on a parametric law between the mean growth rate and the velocity of a high-angle boundary, the model offers valuable insight on the

influence of solute on grain growth. As it is generally believed, the model predicts that the grain growth evolution could be divided into three stages: a impurity independent stage where the boundary is free of a solute atmosphere and a grain growth exponent n close to 2; a transition stage during which the growth rate slows down and the exponent n is larger than 2; and finally an impurity dependent stage where the boundary is fully loaded and the exponent n again approaches a value close to 2.

The model has been applied successfully on experimental grain growth in zone-refined iron, in aluminum alloys and finally in zone-refined lead. These simulations underline the tremendous effect that minute quantities of solute can have on grain growth, and by consequence, the difficulty to carry out grain growth experiments in a controlled manner and the difficulty to interpret them.

ACKNOWLEDGMENTS

The authors would like to acknowledge the financial support from the Research Council of Norway KMB Project No. 193179/I40. The authors extend a very special thanks to Dr. O. Engler for useful discussions and help in solving the computational problems.

OPEN ACCESS

This article is distributed under the terms of the Creative Commons Attribution License which permits any use, distribution, and reproduction in any medium, provided the original author(s) and the source are credited.

REFERENCES

1. P.A. Beck: *Adv. Phys.*, 1954, vol. 3, pp. 245–324.
2. J.E. Burke and D. Turnbull: *Prog. Met. Phys.*, 1952, vol. 3, pp. 220–92.
3. P. Gordon and T.A. El-Bassouini: *Trans. AIME*, 1965, vol. 233, pp. 391–97.
4. H. Hu: *Can. Metall. Q.*, 1974, vol. 13, pp. 275–86.
5. P.A. Beck, J.C. Kremer, L.J. Demer, and M.L. Holzworth: *Trans. AIME*, 1948, vol. 175, pp. 372–400.
6. F. Humphreys and M. Hatherly: *Recrystallization and Related Annealing Phenomena*, Elsevier, Netherlands, 2004.
7. J.W. Cahn: *Acta Metall.*, 1962, vol. 10, pp. 789–98.
8. K. Lücke and H.-P. Stüwe, In *Recovery and Recrystallization of Metals*, L. Himmel, ed., Wiley, New York, NY, 1963, pp. 171–210.
9. K. Lücke and H.P. Stüwe: *Acta Metall.*, 1971, vol. 19, pp. 1087–99.
10. E. Hersent, K. Marthinsen, and E. Nes: *Metall. Mater. Trans. A*, 2013, vol. 44A, pp. 3364–75.
11. E. Hersent, K. Marthinsen, and E. Nes: *Model. Numer. Simul. Mater. Sci.*, 2014, vol. 4, pp. 8–13.
12. P.-R. Cha, S.G. Kim, D.-H. Yeon, and J.-K. Yoon: *Acta Mater.*, 2002, vol. 50, pp. 3817–29.
13. D. Fan, S.P. Chen, and L.Q. Chen: *J. Mater. Res.*, 1999, vol. 14, pp. 1113–23.
14. K. Grönhagen and J. Ågren: *Acta Mater.*, 2007, vol. 55, pp. 955–60.
15. S.G. Kim and Y.B. Park: *Acta Mater.*, 2008, vol. 56, pp. 3739–53.

16. J. Li, J. Wang, and G. Yang: *Acta Mater.*, 2009, vol. 57, pp. 2108–20.
17. G.G. Gottstein and G.G.L.S. Shvindlerman: *Grain Boundary Migration in Metals: Thermodynamics, Kinetics, Applications*, Taylor & Francis Group, 1999, pp. 137–38.
18. H. Westengen and N. Ryum: *Philos. Mag. A*, 1978, vol. 38, pp. 279–95.
19. H.K.D.H. Bhadeshia and R.W.K. Honeycombe: *Steels: Microstructure and Properties*, 3rd ed., Butterworth-Heinemann, Amsterdam, 2006, p. 12.
20. H.-K. Kim, W.-S. Ko, H.-J. Lee, S.G. Kim, and B.-J. Lee: *Scripta Mater.*, 2011, vol. 64, pp. 1152–55.
21. Y. Shibuta, S. Takamoto, and T. Suzuki: *ISIJ Int.*, 2008, vol. 48, pp. 1582–91.
22. D. Wolf: *Philos. Mag. A*, 1990, vol. 62, pp. 447–64.
23. K. Lücke and K. Detert: *Acta Metall.*, 1957, vol. 5, pp. 628–37.
24. F.R. Boutin: *J. Phys. Colloq.*, 1975, vol. 36, pp. 355–65.
25. A. Lens, C. Maurice, and J.H. Driver: *Mater. Sci. Eng. A*, 2005, vol. 403, pp. 144–53.
26. S. Saimoto and H. Jin: in *Fundamentals of Deformation and Annealing*, P.B. Prangnell and Bate P.S., ed., Trans Tech Publications Ltd., Stafa-Zurich, 2007, pp. 339–44.
27. Ø. Ryen, O. Nijs, E. Sjölander, B. Holmedal, H.E. Ekström, and E. Nes: *Metall. Mater. Trans. A*, 2006, vol. 37A, pp. 1999–2006.
28. T. Furu: *Modelling of Recrystallization Applied to Commercial Aluminium Alloys*, Universitetet i Trondheim, Norges tekniske høgskole, Trondheim, 1992.
29. E. Nes and T. Furu: *Scripta Metall. Mater.*, 1995, vol. 33, pp. 87–92.
30. Y. Du, Y.A. Chang, B. Huang, W. Gong, Z. Jin, H. Xu, Z. Yuan, Y. Liu, Y. He, and F.Y. Xie: *Mater. Sci. Eng. A*, 2003, vol. 363, pp. 140–51.
31. P. Gordon and R.A. Vandermeer: *Trans. AIME*, 1962, vol. 224, pp. 917–28.
32. G.F. Bolling and W.C. Winegard: *Acta Metall.*, 1958, vol. 6, pp. 283–87.
33. G.F. Bolling and W.C. Winegard: *Acta Metall.*, 1958, vol. 6, pp. 288–92.
34. J.P. Drolet and A. Galibois: *Acta Metall.*, 1968, vol. 16, pp. 1387–99.
35. J.P. Drolet and A. Galibois: *Metall. Trans.*, 1971, vol. 2, pp. 53–64.
36. E.A. Grey and G.T. Higgins: *Acta Metall.*, 1973, vol. 21, pp. 309–21.
37. K.T. Aust and J.W. Rutter: *Trans. AIME*, 1959, vol. 215, pp. 820–31.
38. K.T. Aust and J.W. Rutter: *Trans. AIME*, 1959, vol. 215, pp. 119–27.
39. T.H. Heumann and J. Johannisson: *Acta Metall.*, 1972, vol. 20, pp. 617–25.
40. W.F. Gale and T.C. Totemeier: *Smithells Metals Reference Book*, 8th ed., Elsevier, 2004, p. 13–26.